Z. Phys. C - Particles and Fields 26, 93–103 (1984)

Zeitschrift für Physik C Particles and Fields

Some Comments on Jet Fragmentation Models and α_s Determinations

Torbjörn Sjöstrand

Deutsches Elektronen-Synchrotron DESY, D-2000 Hamburg 52, Federal Republic of Germany

Received 9 March 1984

Abstract. A number of interrelated topics on jet properties in e^+e^- annihilation is discussed. The need for different α_s values in different fragmentation models is explained, with particular emphasis on the sensitivity to the choice of momentum conservation scheme in independent fragmentation models. Also other factors leading to a broad range of experimental α_s values are discussed. Old and new methods to distinguish different fragmentation models are presented, with particular emphasis on gluon jet fragmentation properties.

1. Introduction

The experimental groups at PETRA and PEP have collected a wealth of data on jets in high energy e^+e^- annihilation events. This way, much has been learned about particle compositions, heavy flavour fragmentation functions, charge correlations, three-jet structures, etc. Despite these advances, the details of jet fragmentation are still fairly poorly known, with no commonly accepted picture emerging so far.

In this paper, we want to discuss some sources of confusion and study possible remedies. First a brief introduction is given to the models so far mostly used to interpret data, the string fragmentation (SF) and independent fragmentation (IF) models (Sect. 2). In particular, the impact of different momentum conservation schemes in IF models is sorted out (Sect. 3). This provides us with an understanding of why different fragmentation models need different α_s values to describe the same data (Sect. 4). As a case example, the energy–energy correlation asymmetry is studied in more detail (Sect. 5). Also uncertainties caused by the use of different matrix element implementations are briefly enumerated (Sect. 6). Finally, the possibility of rejecting some fragmentation models is reviewed, with particular emphasis on the concept of and study of gluon fragmentation (Sect. 7).

Our aim is not to present or interpret experimental data in a quantitative fashion. Rather, we want to point to the qualitative behaviour of data and/or models for some interesting observables. The experimental implications anyhow have to be worked out starting from the actual capabilities of a given detector. To this end, all tools necessary to reproduce the results in this paper are available within the framework of the Lund Monte Carlo (JETSET version 5.2) [1].

2. Fragmentation Models

The Lund model for SF (string fragmentation) has been amply described elsewhere [2, 3], here only a brief summary of the most pertinent features is given. The main idea is to use the massless relativistic string, which provides the simplest causal and Lorentz covariant description of a linear force field, to approximate the linearly confining colour flux tube expected in QCD. The original q and $\bar{q}$ are associated with the endpoints of the string, and gluons are associated with energy and momentum carrying kinks on it. Thus, in a $q\bar{q}g$ event, the string is stretched from the q via the g to the $\bar{q}$. After fragmentation, this will lead to particles lying predominantly along two hyperbolae in momentum space, one in the qg angular range, with the q and g directions as asymptotes, the other correspondingly in the $\bar{q}g$ range. An important and nontrivial feature of the string model is that the fragmentation of a $q\bar{q}g$ event continuously approaches that of a simple $q\bar{q}$ one when the qg or $\bar{q}g$ invariant mass becomes small [3].

The breaking of the string by the production of $q\bar{q}$ pairs is described by the tunnelling mechanism [2]. This leads to the suppression of the production of

heavier flavours, for $s\bar{s}$ by a factor $\sim 1/3$, for $c\bar{c} \sim 10^{-11}$. The same mechanism can be used to give a simple model for baryon production. It also gives a Gaussian $p_\perp$ spectrum, quantified by the parameter $\sigma: \langle p_{\perp q}^2 \rangle = \sigma^2 (= 2\sigma_q^2)$. The distribution of breakup vertices, and hence the sharing of energy and momentum between the produced hadrons, is derived from the principle of left-right symmetry [2]. Since all breakup vertices are causally disconnected, the process can be described recursively. In the simple $q\bar{q}$ case one then obtains a scaling function

$$f(z) = \frac{1}{z}(1-z)_a \, e^{-bm_\perp^2/z} \tag{1}$$

for the fraction z of remaining $E + p_L$ (i.e. energy and longitudinal momentum) taken by a hadron with transverse mass $m_\perp$ (in this paper the term fragmentation function is reserved for the actual particle spectrum obtained by recursive use of the scaling function). The extension of (1) to multijet events is discussed in [3]. The two universal parameters a and b are properly to be determined experimentally. We have chosen to keep $a = 1$ fixed in the following; fits then give $b \approx 0.7\,\mathrm{GeV}^{-2}$ [4]. A main consequence of (1) is that heavy hadrons (charm, bottom) obtain harder fragmentation spectra, $\langle z_{D^*} \rangle \approx 0.56$ and $\langle z_B \rangle \approx 0.82$, in good agreement with experimental data [5].

The most well known IF (independent fragmentation) model is the one presented by Field and Feynman [6] for single u, d and s jets. For applications to e^+e^- annihilation many further components are necessary: charm and bottom fragmentation and decay, gluon jets, QCD matrix elements, etc. Of the many programs written, we restrict our attention to the Hoyer et al. [7] and Ali et al. [8] Monte Carlos, which (in addition to the Lund Monte Carlo) are the only ones to have found extensive experimental use, e.g. for α_s determinations. In the Hoyer model, the gluon is assumed to fragment like a quark of random flavour ($u, d, s, \bar{u}, \bar{d}, \bar{s}$), denoted $g = q$ in the following. Optionally one could use a softer scaling function than for ordinary quark jets (as is actually done in the Hoyer Monte Carlo, although there not much enough to make any real difference), but we will refrain from this here. In the Ali model, the Altarelli–Parisi splitting function [9] is used to divide the gluon energy between a q and a corresponding $\bar{q}$ jet, which then are allowed to fragment independently. This option, $g = q\bar{q}$, thus gives a softer gluon fragmentation function than the $g = q$ one. The (well separated, high energy) Lund gluon actually fragments somewhat softer than the $g = q\bar{q}$ one, since the energy is evenly shared between the two string pieces stretched by the gluon, but basically $g = q$ and $g = q\bar{q}$ may be used to represent "reasonable extremes" for the longitudinal fragmentation properties. The transverse momentum distributions in quark and gluon fragmentation can be chosen independently of each other in IF models (not so in SF, where they are one and the same), but this freedom is used neither here nor in the standard Hoyer and Ali Monte Carlos.

In both the Hoyer and Ali models, the fragmentation is assumed to take place in the hadronic CM frame. This is important because IF is explicitly Lorentz frame dependent, in that a different result would have been obtained had the parton configuration been boosted to another frame, allowed to fragment independently there, and afterwards been boosted back. A more consistent alternative is outlined in [10]: if one assumes separate kinds of quark and gluon "strings", the relevant frame for a $q\bar{q}g$ event is the one where the string tensions exactly balance. Such "IF" models generally tend to give results intermediate to those of the conventional IF ones and the SF one, and will not be considered further here.

3. Momentum Conservation

The concept of IF inevitably leads to the total energy, momentum and flavour not being exactly conserved. For a long time it was thought that this could be corrected for trivially, even to the point that the subject was not even mentioned in model descriptions [7, 8]. We will in the following show why this is not correct.

First consider a massless parton produced with $E = p_L = E_0$. This parton is assumed to fragment independently, so that the massless parton is replaced by a jet with nonzero invariant mass, i.e. $p_L < E$. In the basic procedure of [6], the average jet energy is close to the original parton one, $\langle E \rangle \approx E_0$. The mean p_L value is then given by $\langle p_L \rangle = E_0 - E_m$ where E_m, the average mismatch between energy and momentum, is independent of E_0 for E_0 not too small. Approximately, $E_m \approx \langle m_\perp \rangle / \langle z \rangle$, where $\langle m_\perp \rangle$ is the mean transverse mass of primary hadrons and $\langle z \rangle$ some mean of the scaling variable. This form for E_m can be derived from the assumption of scaling, via the intermediate result that the jet mass-squared grows linearly with the jet energy. A more direct proof is given by the explicit generation of jets, Fig. 1. In particular, a softly fragmenting gluon corresponds to a smaller $\langle z \rangle$ and hence a larger E_m.

For a back-to-back two-jet system, the average longitudinal momentum is decreased by the same amount on both sides, such that the total momentum is conserved on the average. Not so for three-jet events. If the total momentum before fragmentation is vanishing, and if the final jet momenta are parallel with the initial parton momenta, then all initial momenta would have to be scaled down by the same factor to keep total momentum conserved. In IF, however, a fixed amount E_m of momentum is subtracted from each jet, such that the relative change is largest for a low-momentum parton, Fig.

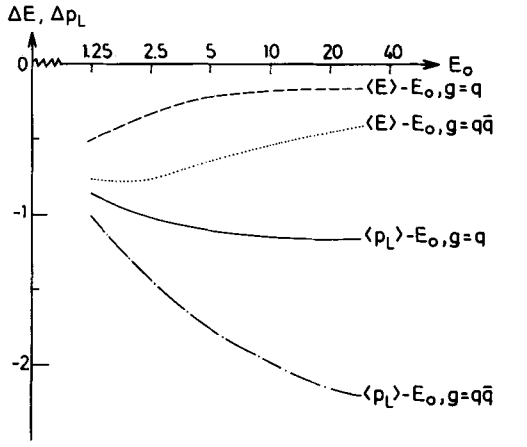

Fig. 1. Energy and momentum (in GeV) "lost" in the independent fragmentation of a gluon jet: full P_L and dashed E for $g = q$, dash-dotted P_L and dotted E for $g = q\bar{q}$

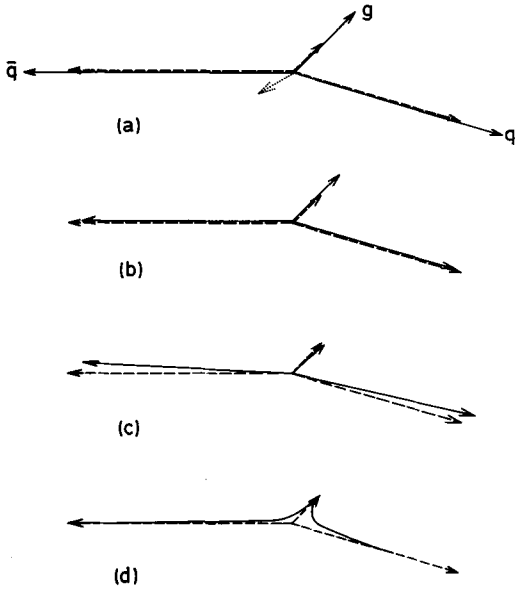

Fig. 2a–d. A slightly exaggerated picture of momentum conservation effects. In **a** the momenta of initial partons are full arrows and of jets after fragmentation dashed, with dotted indicating final momentum imbalance: In **b–d** the momenta before conservation are dashed (as in **a**), after full. Hoyer rescaling in **b**, Ali boost in **c**, Lund strings (along which particles are sitting) in **d**

2a. Thus, the final state net momentum vector $\bar{p}_{\text{imbal}}$ is typically pointing oppositely to the direction of the lowest-energy jet. In the QCD three-jet matrix element this is the gluon one most of the time. Specifically, at $W = 35$ GeV with a matrix element cutoff $y = 0.02$ (i.e. parton–parton invariant masses $m_{jk}^2 > y W^2$), the mean absolute value is $\langle |\bar{p}_{\text{imbal}}| \rangle \approx 1.27$ (1.71) GeV/c and the projection on the gluon direction $\langle \bar{p}_{\text{imbal}} \cdot \bar{p}_g / p_g \rangle \approx -0.75\,(-1.37)$ GeV/c for $g = q\,(g = q\bar{q})$.

The method for momentum conservation adopted in the Hoyer Monte Carlo, in the following denoted $pc = H$, is to conserve transverse momentum locally within each jet, and then rescale longitudinal momenta of particles separately for each jet, such that the ratio of rescaled jet momentum over initial parton momentum is the same for $q, \bar{q}$ and g. The ratio is chosen such that also the correct total energy is obtained. On the average, the effect of momentum conservation then is to significantly scale up longitudinal momenta within the gluon jet, and slightly scale them down for the q and $\bar{q}$ ones, Fig. 2b. This is quantified by the average value of x_g, twice the energy fraction of the gluon or gluon jet, which is 0.354 on the parton level, 0.351(0.339) before and 0.374(0.385) after momentum conservation for $g = q\,(g = q\bar{q})$ and the same W and y values as above. In terms of the energy sharing between the jets, this scheme thus tends to make the events more three-jetlike, whereas angular correlations are kept fixed.

A completely different approach, denoted $pc = A$, was chosen in the Ali Monte Carlo. Given the imbalance $\bar{p}_{\text{imbal}}$ and the total energy E_{tot}, a boost vector $\bar{\beta} = -\bar{p}_{\text{imbal}}/E_{\text{tot}}$ is defined, such that the Lorentz boosted event has vanishing total momentum. (Energy conservation is obtained by rescaling all particle momenta by a common factor afterwards.) The boost then tends to be along the gluon jet direction, such that the q and $\bar{q}$ jets become more back-to-back, Fig. 2c. Defining an acollinearity angle $\Theta_A = 180^\circ - \Theta_{qq}$, $\langle \Theta_A \rangle = 23.6^\circ$ before the boost and $\langle \Theta_A \rangle = 21.9^\circ (20.1^\circ)$ after for $g = q\,(g = q\bar{q})$. The boost also tends to shuffle a bit of energy into the gluon jet, to give $\langle x_g \rangle = 0.356(0.346)$. In angular correlations, the shift is then towards more two-jetlike events, whereas energy sharing between the jets is but little affected.

Four minor comments. Firstly, the importance for α_s measures not only depends on the mean values quoted above, but also on the smearing around these values, since the QCD cross section is rapidly varying. Secondly, an analysis of the effects on four-jets give similar results as for three-jets. Thirdly, many other momentum conservation schemes could be devised; what is more, any "linear" combination of working algorithms will also do. We have tried a few other alternatives, but they tend to give intermediate results, and will not be reported on. Fourthly, we are using results obtained with "emulators" built into the Lund Monte Carlo as options rather than the results from the Hoyer and Ali Monte Carlos themselves. This way we avoid biases from other factors like matrix element treatment etc. Minor differences also exist in the conservation procedures proper, in particular the flavour conservation is handled differently, but a few comparisons [4] give good agreement between the emulators and the Hoyer and Ali programs.

No separate momentum, energy or flavour conservation is necessary in the string case. Rather,

these properties are conserved step by step in the fragmentation process, as given by local conservation of flavour and the (classically described) flow of energy and momentum along the string. The following deliberation may still be helpful. Assume that an IF event were to be "patched up" to resemble a SF one. To describe the effect that particles are distributed around hyperbolae in momentum space, low-momentum particles in the q and $\bar{q}$ jets would then have to be shifted in the g jet direction (and also low-momentum particles in the gluon jet would have to be shifted). This momentum shift would have to behave something like m^2/p_L for a particle with mass m and longitudinal momentum (along q or $\bar{q}$, respectively) p_L, Fig. 2d. It is precisely this shift that also would compensate for the momentum imbalance along the gluon direction.

The difference between SF and IF as to momentum conservation effects is then summarized as follows. In the string model the momenta of fast particles remain unaffected, both in magnitude and direction, and the "joining of jets" is taken care of by low-momentum particles. In the Hoyer and Ali IF models, high-momentum particles are affected most, the momentum change due to a rescaling being proportional to p, of a boost to E.

4. Momentum Conservation Implications for α_s Determinations

As we have seen above, a given implementation of momentum conservation may tend to make events more three-jetlike (Hoyer) or more two-jetlike (Ali, SF). It should therefore come as no surprise that different values for the strong coupling constant α_s are needed to describe experimental data in the different cases [13, 14]. To put this on a more quantitative footing we have generated ~ 25000 events at 35 GeV, using second order QCD formulae with $\alpha_s = 0.16$, $y = 0.02$. Each initial parton configuration was fragmented both in SF and IF fashion, the latter with $g = q$ or $g = q\bar{q}$ and $pc = n$ (no momentum conservation), $pc = H$ or $pc = A$. A number of different event measures were evaluated, all of which supposed to gauge the number of three- (and four-) jet events, with a small background only from two-jets. One, the energy–energy correlation asymmetry EECA will be further discussed in Sect. 5. The others are event shape measures: thrust T, oblateness O, sphericity S, aplanarity A, linear sphericity S', and a cluster method, all using the implementations in [1]. In Table 1 the resulting values are presented, with the IF results normalized to the SF ones.

It is quite clear that differences between different schemes are large, indeed with $pc = H$ giving the most three-jetlike events. Without momentum conservation one ends up somewhere in between $pc = H$ and $pc = A$, but not quite. For the EECA, which is sensitive to the angles between particles, $pc = n$ and $pc = H$ agree fairly well. For event shape measures, $pc = n$ and $pc = A$ are closer to each other, typically because of a balance between particles boosted closer to the jet axis and those boosted away from it. Since the effects of momentum conservation are more accentuated for $g = q\bar{q}$ than for $g = q$, also the gap between $pc = H$ and $pc = A$ is larger in this case (see [2] for a further discussion on gluon softness effects).

The ratios in Table 1 indicate that different α_s values have to be used for different fragmentation models. Further, the results in Table 1 were obtained using the same fragmentation parameters, so that two-jet events were essentially identical in all models. As a check, new "reasonable" α_s values were chosen based on the ratios in Table 1, and the b and σ longitudinal and transverse fragmentation parameters were in each case refitted to give the same mean total multiplicity and aplanarity as in the SF case. The

Table 1 Results for different fragmentation models with second order QCD, $\alpha_s = 0.16$, $y = 0.02$ and fragmentation parameters $b = 0.7\ \mathrm{GeV}^{-2}$, $\sigma = 0.4$ GeV. P(condition) represents fraction of events fulfilling this condition. IF results are normalized to the SF ones, statistical error in the ratios are typically ± 0.03

		IF result/SF result					
event measure	SF result	$g = q$ $pc = n$	$pc = H$	$pc = A$	$g = q\bar{q}$ $p = n$	$pc = H$	$pc = A$
EECA	0.0165	1.79	1.79	1.55	1.67	1.74	1.33
$P(T < 0.85)$	0.133	1.40	1.57	1.37	1.43	1.68	1.40
$P(T < 0.80)$	0.064	1.35	1.47	1.29	1.37	1.66	1.33
$P(T < 0.75)$	0.030	1.25	1.35	1.22	1.30	1.54	1.27
$P(O > 0.15)$	0.147	1.33	1.52	1.29	1.12	1.45	1.05
$P(S' > 0.35)$	0.128	1.36	1.49	1.33	1.38	1.63	1.34
$P(S > 0.2, A < 0.1)$	0.122	1.29	1.46	1.26	1.11	1.43	1.13
$P(\geqq 3$ clusters)	0.120	1.30	1.53	1.32	1.09	1.53	1.16
$P(\tilde{\Theta}^{(0)} > 0.5)$	0.133	1.69	1.73	1.55	1.83	1.75	1.53
$P(\tilde{\Theta}^{(1)} > 0.35)$	0.153	1.52	1.52	1.33	1.57	1.55	1.23
$P(\tilde{\Theta}^{(2)} > 0.35)$	0.153	1.36	1.34	1.19	1.36	1.36	1.08
$P(\tilde{\Theta}^{(4)} > 0.35)$	0.162	1.29	1.28	1.14	1.28	1.30	1.02

Table 2. Results for different fragmentation models if different second order α_s are used and fragmentation parameters are fitted to give same mean multiplicity and aplanarity

parameter, event measure	SF result	IF result/SF result					
		$g = q$			$g = q\bar{q}$		
		$pc = n$	$pc = H$	$pc = A$	$pc = n$	$pc = H$	$pc = A$
α_s	0.16	0.115	0.11	0.125	0.12	0.105	0.135
$b(\mathrm{GeV}^{-2})$	0.7	0.52	0.53	0.61	0.65	0.58	0.74
$\sigma(\mathrm{GeV})$	0.4	0.44	0.44	0.43	0.43	0.44	0.43
EECA	0.0165	1.19	1.17	1.15	1.22	1.07	1.13
$P(T < 0.85)$	0.133	1.06	1.15	1.09	1.08	1.14	1.15
$P(T < 0.80)$	0.064	0.98	1.06	1.03	1.01	1.10	1.15
$P(T < 0.75)$	0.030	0.91	0.94	0.94	0.93	0.98	1.08
$P(O > 0.15)$	0.147	0.84	0.97	0.94	0.80	0.89	0.90
$P(S' > 0.35)$	0.128	1.02	1.10	1.05	1.02	1.09	1.10
$P(S > 0.2, A < 0.1)$	0.122	0.90	1.04	0.99	0.84	0.95	0.94
$P(\geqq 3$ clusters)	0.120	0.86	1.01	1.00	0.80	0.96	0.99
$P(\tilde{\Theta}^{(0)} > 0.5)$	0.133	1.33	1.30	1.32	1.39	1.29	1.35
$P(\tilde{\Theta}^{(1)} > 0.35)$	0.153	1.08	1.03	1.19	1.15	0.99	1.05
$P(\tilde{\Theta}^{(2)} > 0.35)$	0.153	0.94	0.91	0.90	1.01	0.87	0.92
$P(\tilde{\Theta}^{(4)} > 0.35)$	0.162	0.90	0.87	0.85	0.93	0.82	0.87

new ratios are now clustered around 1, as they should, Table 2.

From Tables 1 and 2 it is also clear that not all measures need give an equally large spread in α_s values. One might then hope to construct a measure which would give a unique α_s value, although our experience so far is fairly discouraging. Thus, the cuts on our event measures were chosen to give a remaining three-jet fraction of 10–15%, a compromise between maximizing the statistics and minimizing the two-jet contamination. If harsher cuts are used, the spread is decreased for many measures, as shown for thrust, but not enough to make it worthwhile. A "new" measure was also defined and tested as follows. Use a cluster algorithm [1] linear in momenta, to divide each event into exactly three clusters. Within each cluster j, define an axis for different momentum dependence n by [11]

$$\vec{d}_j^{(n)} = \sum_{i \in j} |\vec{p}_i|^{n-1} \vec{p}_i \tag{2}$$

From these the three opening angles $\Theta_{jk}^{(n)}$ between clusters may be calculated. An event is two-jetlike if some $\Theta_{jk}^{(n)} \sim 0$ or $\sim \pi$. Therefore $\tilde{\Theta}^{(n)}$ is defined by

$$\tilde{\Theta}^{(n)} = \frac{3}{2\pi} \min(\min \Theta_{jk}^{(n)}, 2(\pi - \max \Theta_{jk}^{(n)})) \tag{3}$$

such that $0 \leqq \tilde{\Theta}^{(n)} \leqq 1$, with $\tilde{\Theta}^{(n)} = 1$ corresponding to a symmetric three-jet event. As is seen from Table 1, the construction is such that $g = q$ and $g = q\bar{q}$ come out fairly close, and that the different models become more similar for higher n (up to $n \approx 4$, above that not much happens), i.e. when high-momentum particles are weighted up. This still leaves a sizeable factor 1.3 between the SF case and the most "extreme" IF one.

An increase in energy will bring the models closer together, as shown in Table 3 for the SF and IF ($g = q$, $pc = H$) case, at the same time as the models pull closer to the naive perturbative QCD results. The fragmentation "power corrections" have different fall-off for different measures, as discussed in [12], such that e.g. thrust or $\tilde{\Theta}^{(4)}$ converges much faster than sphericity or $\tilde{\Theta}^{(0)}$. It is doubtful whether the presently available range could be used to estimate the size of these power corrections from data alone, thus providing "model independent" fragmentation corrections. Probably Monte Carlos would still be needed at least to motivate the choice of ansatz for the W dependence. It may also be sobering to realize that, although the situation will be better at LEP, uncertainties of up to 20% will still remain. Probably similar conclusions hold for α_s determinations based on the fraction of events with three high-$p_\perp$ jets at the SPS $p\bar{p}$ collider.

Table 3. Energy dependence of fragmentation model differences. Parameters as for Table 1, specifically $\alpha_s = 0.16$ is taken fixed

event measure	IF ($g = q$, $pc = H$) result/SF result					
	$W =$ (GeV)					
	25	35	60	100	150	250
EECA	1.92	1.79	1.42	1.26	1.18	1.11
$P(T < 0.85)$	1.77	1.57	1.32	1.16	1.12	1.08
$P(T < 0.80)$	1.75	1.47	1.23	1.14	1.11	1.04
$P(T < 0.75)$	1.62	1.35	1.22	1.13	1.08	1.08
$P(O > 0.15)$	1.51	1.52	1.37	1.21	1.15	1.11
$P(S' > 0.35)$	1.75	1.49	1.29	1.15	1.07	1.06
$P(S > 0.2, A < 0.1)$	1.56	1.46	1.32	1.28	1.22	1.29
$P(\geqq 3$ clusters)	1.67	1.53	1.34	1.22	1.12	1.09
$P(\tilde{\Theta}^{(0)} > 0.5)$	1.56	1.73	1.68	1.59	1.55	1.52
$P(\tilde{\Theta}^{(1)} > 0.35)$	1.64	1.52	1.30	1.17	1.14	1.08
$P(\tilde{\Theta}^{(2)} > 0.35)$	1.49	1.34	1.17	1.08	1.04	1.02
$P(\tilde{\Theta}^{(4)} > 0.35)$	1.46	1.28	1.12	1.04	1.02	1.00

Table 4. Recent determinations of α_s in second order QCD. Statistical and systematic errors are not quoted here, typically they are 0.01–0.02 each. The option $pc = O$ [20] is roughly comparable with $pc = A$

group	matrix el., cuts	measure	IF model	α_s(IF)	α_s(SF)
CELLO [14]	FKSS, y	EECA	$g = q, pc = n$	0.12	0.19
			$g = q, pc = H$	0.12	
			$g = q, pc = O$	0.15	
		cluster	$g = q, pc = n$	0.13	0.18
		thrust	$g = q, pc = H$	0.12	
			$g = q, pc = O$	0.13	
JADE [4]	FKSS, y	EECA	$g = q, pc = H$	0.11	0.165
			$g = q\bar{q}, pc = A$	0.14	
MARK J [15, 16]	ERT, (ε, δ)	EECA	$g = q\bar{q}, pc = A$	0.12	0.14
		oblateness	$g = q\bar{q}, pc = A$	0.14	0.16
PLUTO [17]	ERT, (ε, δ)	EECA	$g = q\bar{q}, pc = A$	0.135	0.155
TASSO [18, 19]	FKSS, (ε,δ)	event shape	$g = q, pc = A$	0.16	0.21
		(global fit)	$g = q\bar{q}, pc = A$	0.18	
			$g = q, pc = n$	0.16	

The deliberations presented here about the differences between SF and IF α_s values are in agreement with the pattern observed by the different experimental groups [4, 13–19, 21], Table 4. In particular, we now understand why CELLO obtains a large difference between SF and IF ($g = q, pc = H$) while MARK J observes much smaller differences when comparing SF with IF ($g = q\bar{q}, pc = A$). The experimental studies involve more detailed fits to data, but comparisons with fewer alternatives, and are thus complementary to the model studies presented here.

5. The Energy–Energy Correlation Asymmetry

The Energy–Energy Correlation EEC is defined by [22]:

$$\sum(\Theta) = \frac{1}{n_{\text{evt}}} \sum_{\text{evt}} \sum_{ij} \frac{E_i E_j}{W^2} \delta(\Theta - \Theta_{ij}) \tag{4}$$

where Θ_{ij} is the angle between two particles in the hadronic final state in the CM frame and the δ function is smeared out by using a finite bin size. From this the asymmetry EECA is formed

$$\Delta\sum(\Theta) = \sum(\pi - \Theta) - \sum(\Theta) \tag{5}$$

with $0 \leqq \Theta \leqq \pi/2$. There is a nontrivial correlation between adjacent bins: if two particles form an angle Θ_{ij}, that is probably because they are sitting inside jets approximately separated by this angle, and then other pairs may be expected at nearby angles. Advantages of the EECA include that it does not depend on finding any jet axes or using only a fraction of the events. For α_s determinations, however, it is sensible to limit the comparison to $\pi/5 \leqq \Theta \leqq 2\pi/5$ (as was done in Tables 1–3): below $\pi/5$ correlations inside a jet or between opposite jets dominate, above $2\pi/5$ statistical fluctuations are large (from forming the difference between two almost equally large numbers).

The asymmetry expected from perturbative QCD is

$$\Delta\Sigma^{\text{QCD}}(\Theta) = \frac{\alpha_s}{\pi} f(\Theta)\left(1 + \frac{\alpha_s}{\pi} R_{as}(\Theta)\right) \tag{6}$$

where $f(\Theta)$ is given analytically in [22]. In first order QCD, $R_{as}(\Theta) = -1$, coming from the normalization in (4)

$$\frac{1}{n_{\text{evt}}} \sim \frac{1}{\sigma_{\text{tot}}} \sim \frac{1}{\sigma_0\left(1 + \frac{\alpha_s}{\pi}\right)} \sim \frac{1}{\sigma_0}\left(1 - \frac{\alpha_s}{\pi}\right) \tag{7}$$

For second order QCD, numerical studies have shown that $R_{as}(\Theta) \approx 3$ is a good approximation in the angular range considered here [23, 24].

Fragmentation effects are large at present energies but should die away like $1/W$ (for W not too small). A possible ansatz for the observable asymmetry then is [25]

$$\Delta\Sigma^{\text{obs}}(\Theta) = \Delta\Sigma^{\text{QCD}}(\Theta) \cdot \left(1 - \frac{c}{W}\right) \tag{8}$$

where c turns out to be essentially independent of angle in the range considered by us (not unreasonably, since both the QCD and the observable asymmetry are constrained to vanish linearly when $\Theta \to \pi/2$). A few values in first order QCD are c(SF) ≈ 16.5 [25], $c(g = q, pc = H) \approx -1$ and $c(g = q\bar{q}, pc = A) \approx 10$.

The c values in the IF models may be understood entirely in terms of the shift of jet energies and/or angles discussed in Sect. 3. For the string case, many low-momentum particles are found in the angular ranges between q or $\bar{q}$ and g and few between q and $\bar{q}$. Then the probability to find two particles at small angles is increased while at large angles it is decreased, i.e. the asymmetry is decreased. In principle, if only the asymmetry coming from high-momentum particles were to be considered, and if differences in quark and gluon fragmentation could be neglected or corrected for, the string and $pc = H$ (or $pc = n$) cases would come out fairly close [2]. As it turns out, however, the major contribution to the asymmetry is for at least one of the two particles of a pair having low momentum, $x_p = 2p/W \lesssim 0.1$.

Typically, $\alpha_s^{(1)} \approx 0.25$ in first order QCD in the SF case [13, 4]. In second order, the change in R_{as} from -1 to 3 would then naively correspond to a shift down to $\alpha_s^{(2)} \approx 0.195$. However, this makes no provision for c being different between first and second order. A more general form is

$$\Delta\Sigma^{\text{obs}}(\Theta) = \frac{\alpha_s}{\pi} f(\Theta)\left[\left(1-\frac{\alpha_s}{\pi}\right)\left(1-\frac{c^{(1)}}{W}\right)+4\frac{\alpha_s}{\pi}\left(1-\frac{c^{(2)}}{W}\right)\right] \tag{9}$$

It then turns out that $c^{(2)}$ is significantly smaller than $c^{(1)} = c$ above, e.g. $c^{(2)}(\text{SF}) \approx 5$, $c^{(2)}(g = q, pc = H) \approx -30$, $c^{(2)}(g = q\bar{q}, pc = A) \approx -10$. This is a phenomenon for which we have found no simple explanation. The result anyhow is to shift $\alpha_s^{(2)}$ from 0.195 to 0.175. Further, it should be remembered that $c^{(1)}$ and $c^{(2)}$ are functions of the fragmentation parameters $(b, \sigma, \ldots)$. Specifically, a harder scaling function leads to lower c values in the string case (since the "momentum imbalance" to be compensated by string effects becomes smaller, cf. Sect. 3). A refitting of fragmentation parameters between first and second order may then decrease $\alpha_s^{(2)}$ slightly more.

The asymmetry observed by the JADE group [4] is compared with the string results in Fig. 3. The use of different matrix element cuts y does influence the results in the region $\Theta \leqq 30°$, as will be further discussed in the next section, but not significantly the results in the QCD fit region. This is actually not trivial, since the y cut is not symmetric in angle, such that the low-Θ region of the EEC is more cut off than the high-Θ one [13]. The EECA is one of the few distributions where different groups have presented results corrected for detector acceptance and initial state radiation. A comparison then reveals that e.g. the CELLO results indeed are higher than the JADE ones, as reflected in the different α_s values obtained (Table 4). It remains an open question whether this is just due to statistical fluctuations or reflects systematic uncertainties.

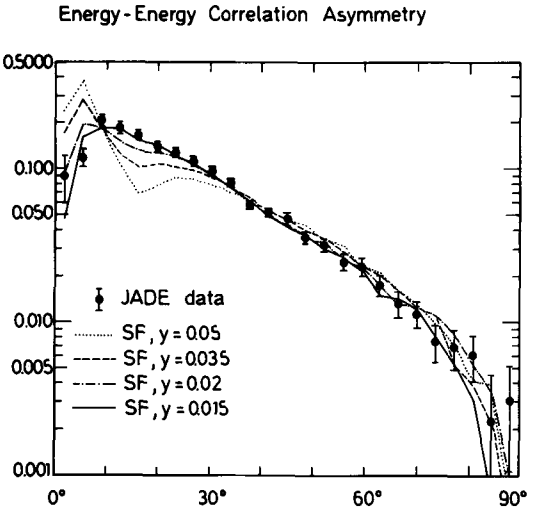

Fig. 3. The Energy–Energy Correlation Asymmetry observed by JADE [4] as filled circles with Lund model results, dotted for $y = 0.05$, dashed for 0.035, dash-dotted for 0.02 and full for 0.015

6. The QCD Matrix Element Implementations

Whereas the $O(\alpha_s)$ three-jet [26] and $O(\alpha_s^2)$ four-jet [27, 28] matrix elements are commonly accepted, there still remains some uncertainty as to the $O(\alpha_s^2)$ contribution to three-jets. We have no original contribution to this subject but, since it is of importance experimentally, we briefly review a few points. First, two different cut procedures are in use for the definition of three- and four-jet events in an infrared safe way. One is the y cut, that for any two partons $m_{jk}^2 = (p_j + p_k)^2 > yW^2$. The other is the (ε, δ) cut, where all partons have energy $E_j > \varepsilon W/2$ and all opening angles $\Theta_{jk} > \delta$ (up to factors of 2 in the definition). Whereas the y cut is explicitly Lorentz covariant, the (ε, δ) cut is to be used in the hadronic CM frame.

The ERT [28] and VGO [29] results have been shown to be equivalent to the FKSS [30] ones for vanishing cut values [31]. For finite cut values, four-jets failing the cuts have to be cancelled against the three-jet virtual correction to give a finite three-jet cross section. The further away from the three-jet singularity a four-jet is, the more the mismatch between three- and four-jet phase space matters. Starting from the ERT formulae, a procedure was worked out [16, 24] (below referred to as ERT + jet resolution) to add vectorially the momenta of the two closest (in invariant mass) partons of a four-jet event to obtain an "equivalent" three-jet one. In the FKSS case, partons outside the δ cones but failing the ε cut are thrown entirely. (In both cases, momenta are rescaled to obtain total energy conservation.) Thus different three-jet events are obtained, generally more two-jetlike in the FKSS case [31]. Therefore a higher α_s may also be necessary in the FKSS case,

which further may depend on the (ε, δ) cut values used [16].

For the y cut case, differences between FKSS and ERT are much smaller, because no partons are thrown away in either case. Remaining discrepancies are mainly constrained to three-jet events close to the two-jet region, where the $O(\alpha_s^2)$ piece of the cross section normally is negative for FKSS and positive for ERT + jet resolution. This is understood as follows. In the FKSS scheme, a four-jet event is reassigned to be a two-jet one if any two of the six parton pairs fail the cut $m_{jk}^2 > y W^2$. The ERT + jet resolution procedure is to first join the two closest partons, and then look at the resulting three-jet. Even if two pairs then are slightly below the cuts in the original four-jet, all three pairs in the three-jet may be above the cuts. (A similar difference appears in the (ε, δ) case.)

Further, some cut regions of phase space, e.g. when the q and $\bar{q}$ of a $q\bar{q}gg$ event are collinear, do not correspond to any matrix element divergences or sensible quantum numbers for a "joined" parton. These are therefore not included in the FKSS three-jet formulae, but would have to be explicitly simulated as four-jets. A final comment: normally massless QCD matrix elements are used, since the $O(\alpha_s^2)$ contributions to the three-jet rate are only available for that case.

Disregarding the uncertainty coming from the use of different fragmentation models, the $\alpha_s^{(2)}$ values for the string model range between 0.14 and 0.21, Table 4. The MARK J and PLUTO groups have been using ERT with (ε, δ) jet resolution cuts, whereas CELLO and JADE have been using FKSS with y cuts. Studies by MARK J [16] and model comparisons between CELLO and MARK J show that the EECA comes out essentially the same in these two cases. The results of the TASSO group were obtained with FKSS and (ε, δ) cuts, and can therefore not be directly compared with those of other groups. The real spread in the data may then be smaller than might be assumed from the spread in α_s values.

Perturbative QCD by itself does not tell which cutoff value should be used, e.g. in terms of y. The EECA study of JADE, Fig. 3 [4], here gives a very interesting hint. In order to get a reasonable agreement with the data at small angles, a very small value has to be used: $y \approx 0.015$ or $m_{ij} \gtrsim 4\,\text{GeV}$. At this point, three- and four-jets essentially saturate the total cross section: $\sim 5\%$ two-jets, $\sim 80\%$ three-jets and $\sim 15\%$ four-jets. Then higher orders in α_s are no longer negligible, so one should not take the exact value $y \approx 0.015$ too seriously. What seems clear is that a sizeable fraction of all "simple" jets indeed contain a jet substructure, and that the fraction of "true" two-jets is small.

Higher orders may also be needed to describe the experimental four-jet rate, which seems to be higher than implied by the second order QCD formulae, both in terms of the out-of-the-plane momentum and the number of four-clusters reconstructed [19, 32, 33] (for IF models only the numbers of four-clusters poses problems [19]). This is not surprising, insofar as the running coupling constant $\alpha_s(Q^2)$ is evaluated at $Q^2 = W^2$. It is well known that a more proper value for three-jets would be $(1-T)W^2 = m_{qg}^2$, i.e. the mass-squared of the off-mass-shell parton propagator. In second order, this ambiguity is removed for three-jets by the appearance of logarithmic terms, which can be interpreted as coming from a series expansion of $\alpha_s((1-T)W^2)$ in terms of $\alpha_s(W^2)$ [28, 34]. In higher orders, a corresponding phenomenon may be expected for four-jets. If the arguments of α_s^2 are changed to better represent the invariant parton masses in the problem (this is not always unique, since different parton cascades may result in the same final parton configuration), this corresponds to a change of weights for different four-jets by a factor between 1.3 and 2.3, with mean ~ 1.7, for $\alpha_s(W^2) = 0.16$ and $y = 0.02$. As a first attempt, one could then increase the four-jet cross section uniformly by a factor $1.5 - 2$ (with the same shift in the "counterterm" in the three-jet cross section necessary for consistency, although less important in practice).

7. Possible Evidence for the String Picture

So far, we have tried to identify the various sources that are responsible for the large spread of α_s values, but not to reduce the allowed range. The most obvious possibility would be to exclude some fragmentation models using the experimental data. Objections could be raised that the range of possible models to be tested is infinite; methods that differentiate between present-day models would still put severe constraints on future model builders. Generally measures that do not depend on identifying the individual jets, such as those used to determine α_s, are the ones that show the largest variation between different models. If the gluon jet in three-jets has to be identified, the possibility to observe string effects is then limited by the impurity of the sample, i.e. the fraction of events which really are two-jets (notably $b\bar{b}$), or four-jets, or where the gluon jet has been misidentified. The ultimate goal, to show whether particles are "distributed along strings" on an event-by-basis, seems to be a very difficult endeavour; so far we have failed to find a good way of achieving this.

A number of tests have been carried out to distinguish SF and IF, notably by the JADE group [35]. So far, this experimental evidence supports the string picture and show several disagreements with the IF ($pc = H$) model, also when the gluon fragmentation is varied. The basic philosophy of JADE is to select for three-jet events and identify the three jet axes, where the jet with the smallest energy is expected to contain an enriched sample of gluon jets. It then turns out that the region between

the q and $\bar{q}$ is depleted from particles compared to the region between q and g. In particular, the effect is increased if one looks at energy flow rather than particle flow, or looks at kaons only, or looks at particles with out-of-the-plane momenta $p_\perp^{\text{out}} > 0.3$ GeV. In the string picture, this pattern naturally follows from the kinematics of the boost between the rest frame of the string piece and the hadronic CM frame.

With respect to the true parton direction, high momentum particles are sitting along the axis in SF (on the average), whereas low momentum particles in a q jet are systematically displaced towards the g side. This difference between high and low momenta can be used in a number of ways. Thus, an experimentally determined q jet axis is normally shifted slightly in the g direction for SF, such that high momentum particles now tend to sit on the $\bar{q}$ side and low momentum ones still on the g side. Again, this behaviour is observed by JADE [35]. Another method, not depending on identifying the gluon jet, is the variation with n of the $\tilde{\Theta}^{(n)}$ measures in Sect. 4. The ratio $P(\tilde{\Theta}^{(4)} > 0.35)/P(\tilde{\Theta}^{(0)} > 0.5)$ is 1.22 for SF and 0.81–0.93 before (Table 1) and 0.77–0.82 after (Table 2) refitting fragmentation parameters for IF. The relatively small spread between different IF schemes is due to the α_s dependence being roughly divided out in the ratio, so that the important feature is the IF picture of jets "sticking out as straight rods from the origin" (which, to first order, is also true in a boost of the event). Other ways this difference has been explored include a CELLO study of cluster thrust using cluster directions found as in (2) [36], a JADE study of the weighted distribution of particle angles with respect to the jet axis [35], and a PLUTO study of the EECA for cluster axes reconstructed from particles with momenta above and below 2.5 GeV as well as the angle between clusters for different particle momentum weight [37].

Another difference noted between SF and IF, is that the former qualitatively can explain the dip of particle density around rapidity $Y = 0$ [38, 39]. This is again related to the string effect pulling out particles from small momenta, such that in three-jet events the density dn/dY of the "broad jet" only reaches its plateau value a bit away from $Y = 0$ [39], whereas IF jets are abruptly cut off at $p_L = 0$.

A very interesting discrepancy in the study of gluon jet fragmentation is that the JADE group, in a study of three-jets ($\sim 10\%$ of the total event sample), favour a softly fragmentation gluon jet [35], something like our $g = q\bar{q}$, whereas the TASSO global fits to all events favour a $g = q$ option [19]. When using SF, on the other hand, both groups find decent agreement with their data. This may be understood as follows. For high energy partons, well separated in angle, the overall picture in SF is not that different from what is obtained in an IF model with a softly fragmenting gluon, with string effects

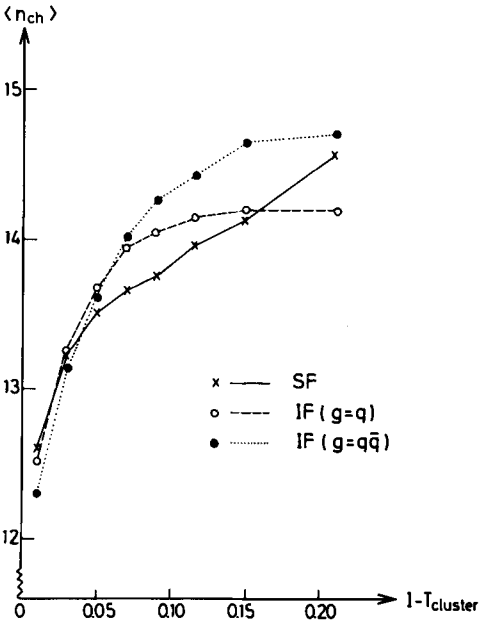

Fig. 4. The mean charged multiplicity as a function of cluster thrust for charged particles. Crosses are for SF, open circles for IF($g = q$) and filled circles for IF($g = q\bar{q}$); lines are drawn to guide the eye

mostly affecting low momentum particles between the jets. Now, when the angle between two partons is decreased, the two resulting jets will begin to merge, as string effects become more and more pronounced, also for high momentum particles. In the limit of collinear partons, the fragmentation will proceed as were there only one parton (q instead of qg, g instead of gg), as discussed in detail in [3]. For the q and g of a $q\bar{q}g$ event fairly close, it therefore does not make sense to speak of the separate fragmentation behaviour of the two. If this is done anyhow, one is forced to have a hard fragmentation function for gluon jets, even harder than the normal quark one, in order to come anywhere near the string description. In a global fit to the data, the averaging between soft and hard gluon fragmentation functions may then give something best described by the $g = q$ option for the IF case.

Since this strikes at the very concept of fragmentation proceeding independently in the different jets, a more direct test should be performed. The continuous collapse of a $q\bar{q}g$ event into a $q\bar{q}$ one when the qg (or $\bar{q}g$) invariant mass vanishes, reflects itself e.g. in the multiplicity. Considered as a function of the true parton thrust ($1 - T_p = m_{qg}^2/W^2$ for $m_{qg} < m_{\bar{q}g}, m_{q\bar{q}}$), the SF multiplicity rises continuously from the two-jet value when T_p is decreased from unity. In IF models, the multiplicity makes an abrupt jump when going from two- to three-jet events, but then stays more constant. This is illustrated in Fig. 4, showing the charged multiplicity as a function of cluster thrust (determined by reconstruct-

ing exactly three clusters from the charged particles, and then using the angles between these). A few comments. The choice of momentum conservation scheme does not significantly affect the results obtained, the IF curves shown actually are mean values of $pc = H$ and $pc = A$. The difference between $g = q$ and $g = q\bar{q}$ is clearly visible; the latter naturally showing a much larger variation with T_{cluster}. As usual, the true effects (before smearing from cluster reconstruction errors etc.) are larger, and more efficient methods could be devised. In particular, it is for collinear gluons rather than for soft ones that the IF and SF descriptions differ most. Therefore suitable cuts on minimum cluster energy could enhance the signal, at the cost of no longer being able to use all the events. Finally, the quantitative behaviour may depend on the exact form of the matrix element cuts, particularly for IF, but this should not affect the qualitative pattern.

Obviously the multiplicity analysis described above is only a foray into a potentially rich field of study. With events binned in cluster thrust, or some other similar measure, one could try to study the fragmentation properties necessary to describe each bin by itself, and also tell something about what is right and wrong with a given model. With jets ordered according to energy, the effects on quark and gluon jets could be partly disentangled. Quark jets alone could also be studied by looking e.g. at the mean energy fraction taken by charm mesons, which shows the same kind of abrupt jump between two- and three-jets in IF models as the multiplicity does.

8. Conclusions

As we have seen, the very large spread of α_s values in e^+e^- annihilation does not have one single cause, but three. One is obviously experimental errors, statistical and systematic. Another is the choice of second order QCD matrix element treatment. The most important source of all, however, is that different fragmentation models need different α_s values to fit the same data. We have in this paper discussed differences between the Lund string model and independent fragmentation models, in particular with respect to the gluon fragmentation and momentum conservation schemes adopted in the latter models. The effects of various choices here are now well understood, at least in broad terms, and one could even set up "conversion tables" for the α_s values in various models, with the proviso that these tables would depend on the measure used.

This fragmentation model dependence may be disappointing to people who want to have all of QCD neatly compressed into one single number. We prefer to think [redacted] as a blessing in disguise, in the sense of provi[redacted]one further reason why the study of fragmentat[redacted]operties, i.e. the nonperturbative effects of QC[redacted]b essential. We have also tried to show that the situation is not hopeless: there are methods, both tried and untried, of distinguishing different fragmentation models.

In this paper we have concentrated on models used in α_s determinations up till now. Obviously this is only a small fraction of the total number of models. A different approach is e.g. adopted in models based on parton cascades followed by cluster decays [40]. The α_s or Λ values extracted from these programs cannot be directly compared with the ones in Table 4, since the matrix elements are somewhat different, even for three-jets. Therefore, comparisons with such models would have to include a separation of matrix element and fragmentation model differences. Several of the methods discussed above could still provide valuable information on the performance of a program. We conclude by a reminder that, whereas some models are more successful than others in describing experimental data, certainly none is perfect. A successful model should therefore be considered as a vehicle for a better understanding of (perturbative and nonperturbative) QCD rather than as a goal by itself.

Acknowledgements. This paper owes much to discussions with and inspiration from a large number of people at DESY, although the opinions expressed obviously are our own. Special thanks go to G. D'Agostini, F. Barreiro, W. de Boer, G. Kramer, A. Petersen, G. Rudolph, G. Schierholz, T. Walsh and R.-Y. Zhu. The hospitality of the DESY Directorate and Theory Group is gratefully acknowledged, in particular we express our thanks to Profs. P. Söding and F. Gutbrod.

References

1. T. Sjöstrand: Comput. Phys. Commun. **27**, 243 (1982); ibid. **28**, 229 (1983)
2. B. Andersson, G. Gustafson, G. Ingelman, T. Sjöstrand: Phys. Rep. **97**, 33 (1983)
3. T. Sjöstrand: DESY 84-019 and internal report DESY T-84-01
4. JADE Collab. A. Petersen et al.: private communication
5. P. Söding: DESY 83-104, talk presented at the Brighton Conference 1983; J. Dorfan: SLAC-PUB-3250, talk presented at the Cornell Conference 1983
6. R.D. Field, R.P. Feynman: Nucl. Phys. **B136**, 1 (1978)
7. P. Hoyer et al.: Nucl. Phys. **B161**, 349 (1979)
8. A. Ali, E. Pietarinen, G. Kramer, J. Willrodt: Phys. Lett. **93B**, 155 (1980)
9. G. Altarelli, G. Parisi: Nucl. Phys. **B126**, 298 (1977)
10. I. Montvay: Phys. Lett. **84B**, 331 (1979)
11. B. Andersson, G. Gustafson, T. Sjöstrand: Phys. Lett. **94B**, 211 (1980)
12. T.F. Walsh: talk presented at the Brighton Conference 1983
13. CELLO Collab., H.-J. Behrend et al.: Nucl. Phys. **B218**, 269 (1983)
14. CELLO Collab., H.-J. Behrend et al.: DESY 83–127
15. MARK J Collab., D.P. Barber et al.: Phys. Rev. Lett. **50**, 2051 (1983)
16. R.-Y. Zhu: Ph.D. thesis (MIT, November 1983)
17. PLUTO Collab., F. Barreiro et al.: private communication
18. G. Wolf: DESY 83–096
19. TASSO Collab., G. Rudolph et al.: private communication
20. R. Odorico: Comput. Phys. Commun. **24**, 73 (1981)
21. K. Stupperich: Ph.D. thesis, DESY PLUTO-83-03; K.-H. Pape: Ph.D. thesis, DESY PLUTO-83-08

22. C. Basham, L. Brown, S. Ellis, S. Love: Phys. Rev. Lett. **41**, 1585 (1978); Phys. Rev. **D19**, 2018 (1979); Phys. Rev. **D24**, 2382 (1981)
23. D.G. Richards, W.J. Stirling, S.D. Ellis: Phys. Lett. **119B**, 193 (1982)
24. A. Ali, F. Barreiro: Phys. Lett. **118B**, 155 (1982); DESY 83-070
25. S.D. Ellis: Phys. Lett. **117B**, 333 (1982)
26. J. Ellis, M.K. Gaillard, G.G. Ross: Nucl. Phys. **B111**, 253 (1976); B.L. Ioffe: Phys. Lett. **78B**, 277 (1978)
27. A. Ali et al.: Nucl. Phys. **B167**, 454 (1980); K.J.F. Gaemers, J.A.M. Vermaseren: Z. Phys. C—Particles and Fields **7**, 81 (1980)
28. R.K. Ellis, D.A. Ross, A.E. Terrano: Nucl. Phys. **B178**, 421 (1981)
29. J.A.M. Vermaseren, K.J.F. Gaemers, S.J. Oldham: Nucl. Phys. **B187**, 301 (1981)
30. K. Fabricius, G. Kramer, G. Schierholz, I. Schmitt: Z. Phys. C—Particles and Fields **11**, 315 (1982)
31. T. Gottschalk: Phys. Lett. **109B**, 331 (1982); F. Gutbrod, G. Kramer, G. Schierholz: Z. Phys. C—Particles and Fields **21**, 235 (1984)
32. JADE Collab., S. Bethke et al.: private communication
33. MARK J Collab., R.-Y. Zhu et al.: private communication
34. Kunszt, Z.: Phys. Lett. **99B**, 429 (1981)
35. JADE Collab., W. Bartel et al.: Phys. Lett. **101B**, 129 (1981); JADE Collab., W. Bartel et al.: Z. Phys. C—Particles and Fields **21**, 37 (1983)
36. CELLO Collab., G. D'Agostini et al.: private communication
37. PLUTO Collab., H. Maxeiner et al.: private communication
38. TASSO Collab., M. Althoff et al.: DESY 83–130
39. JADE Collab., P. Warming et al.: private communication
40. T. Gottschalk: Nucl. Phys. **B214**, 201 (1983); B.R. Webber: TH. 3713-CERN